CONCEPTUAL ELECTROMAGNETIC DESIGN OF A MAGNETISED HADRON STOPPER FOR THE BDF/SHIP EXPERIMENT AT CERN

V. Ferrentino*, M. Liebsch, D. Schoerling, P. Schwarz
CERN, Meyrin, Switzerland

Abstract

The discovery of the Higgs boson marked a major milestone for the Standard Model of particle physics. Nevertheless, several open questions remain, including the nature of dark matter, neutrino oscillations and baryon asymmetry of the universe. Many theoretical models predict new, yet undiscovered particles; however, their detection remains highly challenging due to their weak interactions with ordinary matter. In this context, the SHiP experiment at CERN aims to explore feebly interacting long-lived particles. This paper presents the electromagnetic design of a magnetised hadron stopper for SHiP, required to absorb residual secondary particles from the hadronic shower and providing dipole strength to deflect muons trajectories. The design is particularly challenging due to the high-radiation environment, stringent spatial constraints, and demanding magnetic field requirements. The magnetic design is developed and validated using finite-element models. The results prove that the proposed design meets the magnetic requirements while ensuring flexibility for manufacturing and maintenance, and support the development of a reduced-scale prototype.

INTRODUCTION

The Magnetised Hadron Stopper (MHS) is part of the Beam Dump Facility (BDF) upgrade [1, 2] within the High Intensity upgrade for the ECN3 North Experimental Area (HI-ECN3) of the Super Proton Synchrotron (SPS) at CERN [3,4]. It is a key element of the Muon Shield (MS) [5] for the Search for Hidden Particles (SHiP) experiment foreseen to be installed there. Figure 1 shows the layout of the BDF target station, with the MHS highlighted by the orange rectangle. It fulfills two primary functions: it absorbs residual secondary particles from the hadronic shower induced by the proton beam interaction with the target and initiates the deflection of the muon flux away from the SHiP detector acceptance. The MHS electromagnetic design poses significant challenges. A compact geometry is required to facilitate manufacturing, installation and maintenance. To sufficiently deflect muons with momenta up to 350 GeV/c, a magnetic flux density of 1.9 T is needed. In addition, the proximity to the target vessel exposes the MHS to high radiation levels, demanding a challenging coil design to enable reliable operation over the 15 years of data taking foreseen for the experiment. This paper presents the electromagnetic design of the MHS, optimised to achieve the target magnetic flux density while meeting spatial constraints and limiting manufacturing and operational costs. The 2D cross-section and the coil design are presented and validated through 2D and 3D Finite-Element (FE) simulations. To enable intervention on the coil in case of failure, a careful optimisation of the magnetic circuit to limit residual magnetization and the associated magnetic forces is also performed.

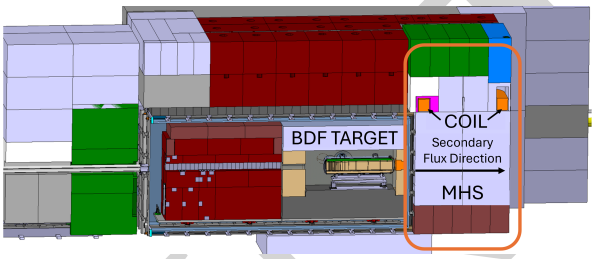

Figure 1: MS complex layout [5].

MHS GEOMETRY

The MHS is an unconventional magnet as it does not require a central aperture. The design follows an install-and-forget philosophy, with coil failure representing the only potential intervention (a part from disposal). The MHS is manufactured with adjacent blocks to facilitate manufacturing, transport and installation. The 2D cross-section of the magnet is shown in Fig. 2. The core (dark blue) is made of high-purity ultra-low-carbon steel (XC06) [6], with transverse dimensions of 0.8 m × 0.8 m ($w_0 \times h_0$). Its centre corresponds to the beam axis. This material and its geometry are selected to concentrate the magnetic flux in the core, enabling the 1.9 T target field to be achieved. To reduce manufacturing costs, the return yoke (light blue) is assembled from 1010 steel, which still provides adequate permeability. The coil region (red) includes conductors, inter-turn and ground insulation. To limit ionizing radiation damage, the coil is positioned at 1.7 m from the beam axis. The iron block between the coil windings is also made of XC06 to mitigate local saturation. Green areas consist of non-magnetic steel.

While the yoke is normally demagnetised before intervention, this may not be possible in the event of a complete failure of the coil. Thus, non-magnetic sheets (black) are placed between the coil insert and the uppermost block to enable removal of the upper yoke block under residual magnetisation. To control the residual field and ensure manageable magnetic forces during lifting, the thickness of the non-magnetic sheet is $g_{a,m} = 6$ mm. 1 mm air gaps (g_a) are also included to account for contact imperfections between adjacent iron blocks, increasing the reluctance of the magnetic circuit. The return yoke block widths (ω_1, ω_2 and ω_3),

* email: vittorio.ferrentino@cern.ch

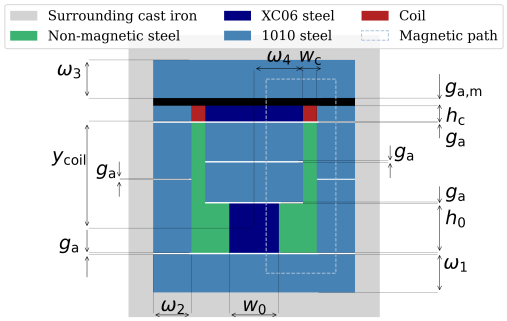

Figure 2: MHS 2D cross-section. XC06 and 1010 steel in dark and light blue, respectively, non-magnetic steel in green, coil in red. Dimension of the air gaps not to scale.

selected to limit saturation and satisfy spatial constraints, is 0.615 m. The MHS longitudinal length, l_m, is 2.3 m. Table 1 summarizes the MHS parameters.

Table 1: MHS 2D Cross-Sectional Parameters

Parameter	Value	Unit
Core width × height, $w_0 \times h_0$	0.8×0.8	m^2
Coil width × height, $w_c \times h_c$	0.225×0.255	m^2
Coil distance to core, y_{coil}	1.7	m
Return yoke, ω_1, ω_2, ω_3	0.615	m
Coil-to-coil distance, $2\omega_4$	1.58	m
Sheet thickness, $g_{a,m}$	6	mm
Surface contact air gaps, g_a	1	mm
Longitudinal length, l_m	2.3	m

COIL DESIGN

With the proposed geometry, a magnetomotive force of 44 000 A turns is required to achieve the target flux of 1.9 T in the centre of the MHS core. This, with the limited space for the coils, requires a current density above 1 A/mm^2, motivating the use of water-cooled conductors. The coil design features 8 double-pancakes connected in series, with one cooling circuit each. One double-pancake consists of 2 layers of 15 turns each. The winding, shown in Fig. 3 in red, results in a total of 240 turns. A square conductor of 12 mm×12 mm with a circular 8.5 mm diameter cooling hole is selected. To provide the required magnetomotive force (44 000 A turns), the coil operates at 183.3 A. This can be maintained even in the case of a 50 % failure of turns by doubling the current to 367.7 A and blocking off the faulty pancakes. The Polaris 2P power converter [7] is selected to supply the MHS coils, providing a maximum current of 500 A with 100 kW maximum power. The electrical and cooling parameters under nominal and failure conditions, computed following [8, 9] and summarised in Table 2, are compatible with the operational requirements and existing cooling infrastructure. Due to space constraints in the MS complex, the coil is fully inserted in the MHS yoke assembly, as illustrated in Fig. 3, resulting in an increased flux density in the coil insert.

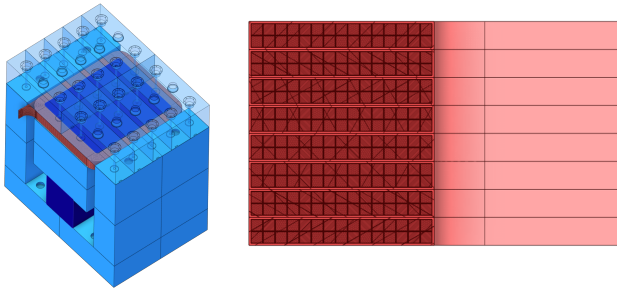

Figure 3: 3D MHS view from the top (left) and 2D cross-section of the coil (right). Coil insert as modeled in the mechanical design. Ceiling blocks displayed transparently

Table 2: Electrical And Cooling Parameters In Nominal And Failure Operation.

Parameter	Nom. Op.	Fail. Op.	Unit
Operating current, I_{op}	183.3	367.7	A
Current density, j	2.1	4.2	A/mm^2
Max. T rise, ΔT	15	30	°C
Average coil T, T_{avg}	32.5	40	°C
Coil resistance, $R_c(T_{avg})$	386	197	mΩ
Inductance, L_c	10.3	2.56	H
Joule power loss, $P_{j,c}$	13.0	26.4	kW
Hydraulic circuits, n_{hy}	8	4	–
Water flow rate, Q_w	1.55	3.78	l/min
Water velocity, v_w	0.45	1.11	m/s
Pressure drop, Δp	1.15	5.51	bar
Reynolds number, Re	5.9×10^3	1.4×10^4	–

FINITE-ELEMENT MODELING

Magnetostatic simulations of the MHS were performed using Opera-2D/3D [10] FE models. The magnetic design was conducted through 2D cross-section optimization to determine the main geometrical parameters, evaluate the transfer function, and assess sensitivity to air-gap variations and mesh-induced numerical errors. 3D simulations were conducted to assess the flux compression in the coil insert. The coils were modeled as current-carrying rectangular regions, including inter-turn insulation, thereby neglecting conductor spacing effects. The cross-sectional dimensions of the FE MHS model correspond to those reported in Table 1. The magnetic steel was assumed to be isotropic. Non-magnetic stainless-steel regions (green in Fig. 1) were modeled as air. 2D FE simulations showed that a magnetomotive force of 38 000 A turns was sufficient to achieve the target flux. The resulting 2D magnetic flux density distribution and field lines are illustrated in Fig. 4, on the left. The core operates at approximately 1.9 T, while the return yoke reaches about 1.6 T, remaining below saturation. The XC06 block between the coil (blue in Fig. 1) operates at approximately 1.2 T. These results confirm that flux is concentrated within the core, validating the flux-compression design principle. In the core region, a vertical dipolar field is generated, providing a horizontal deflection to the muons. In the upper stainless-steel area the leakage fields could be exploited for

the integration of diagnostics.3D simulations were carried out to quantify the effect of flux compression in the coil insert. A magnetomotive force of 44 000 A turns was needed to achieve the target magnetic flux. The 2D magnetic flux density map from the 3D simulation at $z = 0$ is reported on the right in Fig. 4. Compared to the 2D model (on the left), with the same field in the core centre ($B_0 = 1.9$ T), a higher magnetic flux is observed in the upper XC06 block due to the flux compression caused by the coil insert. The MHS transfer function was defined as the variation of the central field, B_0, with magnetomotive force. Fig. 5 compares the 2D and 3D results (blue and green curves, respectively). For a given excitation, the 3D model yields a lower central field due to higher reluctance from the coil insert. Therefore, the target field is reached at approximately 38 000 A turns in 2D, while 44 000 A turns are needed in 3D.The FE analysis confirms that the electromagnetic design of the MHS meets the experimental requirements, while providing operational margin for tuning and fault scenarios.

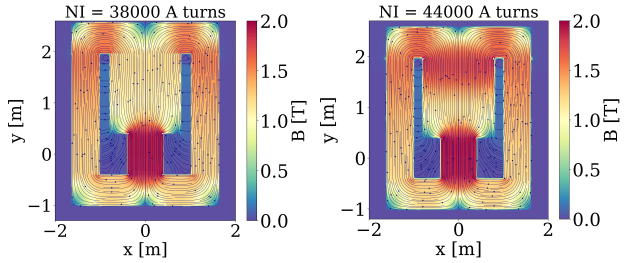

Figure 4: 2D magnetic flux density map and field lines in the MHS from 2D (left) and 3D (right) simulations.

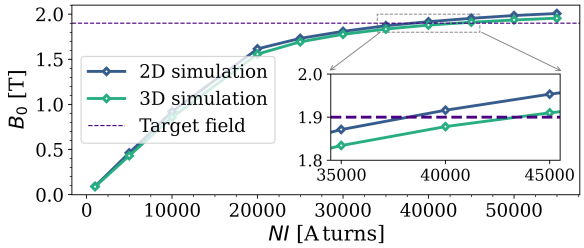

Figure 5: MHS 2D (blue) and 3D (green) transfer functions.

RESIDUAL MAGNETISATION STUDIES

The residual magnetic field in a dipole magnet with a total air gap g can be estimated using the scaling law [8]:

$$B_{\text{res}} = \left(\frac{l_{\text{m}}}{g}\right) \mu_0 H_{\text{c}} \qquad (1)$$

where l_{m} is the average magnetic path length in the iron, and H_{c} is the coercive field of the magnetic material. In this case, the average magnetic path length is approximately 8.5 m (under the assumption that it remains unchanged for the remanent field), while the total air gap amounts to 12 mm, including only the main gap, corresponding to a ratio g/l_{m} of 1.4×10^{-3}. With a conservative H_{c} value for AISI 1010 steel of 200 A/m, a resulting residual magnetic flux density in the

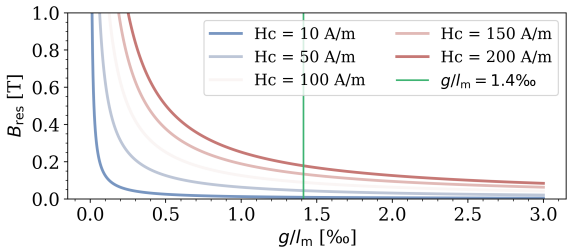

Figure 6: Residual field at different values of H_{c} versus the g/l_{m} ratio in per mill, computed with Eq.((1)).

gap of approximately $B_{\text{res}} = 0.18$ T can be extrapolated from Fig. 6, illustrating Eq.(1). By splitting the uppermost part of the MHS in 10 blocks (as shown in Fig. 3), the magnetic force acting on a surface of area $A = 0.75$ m^2 is:

$$F_{\text{mag}} = \frac{B_{\text{res}}^2}{2\mu_0} A = \frac{0.18^2}{2 \cdot 4\pi \cdot 10^{-7}} \cdot 0.75 \approx 9.7\,\text{kN} \qquad (2)$$

In addition, the gravitational force of a block with volume $V = (1.63 \times 0.46 \times 0.615)$ m^3 ≈ 0.46 m^3 is:

$$F_{\text{g}} = gV\rho = 9.81 \cdot 0.46 \cdot 7.87 \cdot 10^3 \ \text{N} \approx 35.5\,\text{kN} \qquad (3)$$

with $\rho = 7.87$ g/cm^3 the steel density. The total lifting force needed to overcome both gravity and magnetic attraction is therefore 45 kN. In practice, to apply a safety factor and account for friction between adjacent blocks, two hydraulic cylinders with 50 kN lifting capacity each are employed.

CONCLUSION

The Magnetised Hadron Stopper (MHS) is the first element in the SHiP MS complex and is required both to absorb the hadronic shower produced by the SPS proton beam interaction with the target and to initiate the deflection of the muon flux. The MHS electromagnetic design is challenging due to the high-radiation environment, stringent spatial constraints, and the high dipolar magnetic flux density needed. The cross-section is optimised to concentrate the magnetic flux in the core while limiting saturation in the return yoke. The coil is designed to ensure safe operation even in the event of a 50 % failure of coil turns. The resulting electrical and cooling parameters remain within standard values for warm magnets. 2D and 3D FE simulations confirm that the design meets the target magnetic field specifications. To enable coil disassembly without prior demagnetisation, the magnetic circuit and upper yoke structure are designed in such a way as to control residual magnetisation and associated forces. These are kept within manageable limits, allowing safe lifting using appropriate hydraulic cylinders. The results support the feasibility of the proposed design and will inform the development of a reduced-scale prototype to enable material characterization and validation of the flux compression principle and lifting forces.

ACKNOWLEDGMENTS

The authors want to thank all the people within the SHiP - MS project for their valuable and fruitful collaboration.

REFERENCES

[1] E. Lopez Sola *et al.*, "Design of a high power production target for the beam dump facility at CERN", *Phys. Rev. Accel. Beams*, vol. 22, p. 113001, 2019. doi:10.1103/PhysRevAccelBeams.22.113001

[2] K. Kershaw *et al.*, "Design development for the Beam Dump Facility target complex at CERN", *JINST*, vol. 13, p. P10011, 2018. doi:10.1088/1748-0221/13/10/P10011

[3] M. A. Fraser *et al.*, "Investigating the feasibility of delivering higher intensity proton beams to ECN3 at the CERN SPS North Area", in *Proc. IPAC'23*, Venice, Italy, May 2023, pp. 229–232. doi:10.18429/JACoW-IPAC2023-MOPA084

[4] M. A. Fraser, C. Ahdida, *et al.*, "The High Intensity ECN3 Project and the SPS Beam Dump Facility at CERN", presented at IPAC'26, Deauville, France, May 2026, paper THP4061, this conference.

[5] J.-L. Grenard, "BDF/SHiP magnetised hadron stopper", CERN, Geneva, Switzerland, EDMS document 3233771, version 1.0, 2025.

[6] ArcelorMittal, "XC06 XCarb: High-purity ultra-low-carbon magnet steel", technical data sheet, 2026.

[7] CERN Medium Power Converter Section, "POLARIS", CERN, Geneva, Switzerland.

[8] T. Zickler, "Basic design and engineering of normal-conducting, iron-dominated electromagnets", 2011, arXiv:1103.1119 [physics.acc-ph]. doi:10.48550/arXiv.1103.1119

[9] G. de Rijk, "Warm magnets", 2021, arXiv:2107.03965 [physics.acc-ph]. doi:10.48550/arXiv.2107.03965

[10] Dassault Systèmes, "Opera electromagnetic and electromechanical simulation", SIMULIA Opera software.